Tunable fractional-order differentiator using an electrically tuned silicon-on-isolator Mach-Zehnder interferometer

Aoling Zheng,[1,3] Ting Yang,[1,3] Xi Xiao,[2] Qi Yang,[2] Xinliang Zhang,[1] and Jianji Dong[1,*]

[1]*Wuhan National Lab for Optoelectronics, Huazhong University of Science and Technology, Wuhan, 430074, China*
[2]*State Key Laboratory of Optical Communication Technologies and Networks, Wuhan Research Institute of Posts & Telecommunications, Wuhan, 430074, China*
[3]*These authors contributed equally to this work*
[*]*jjdong@mail.hust.edu.cn*

Abstract: We propose and experimentally demonstrate a tunable fractional order photonic differentiator using an on-chip electrically tuned Mach-Zehnder interferometer (MZI) structure. The phase shift at the resonant frequency of the MZI varies when applying different voltages, which can implement the fractional differentiation. Due to the large 3-dB bandwidth of the MZI, the differentiator is expected to have an operation bandwidth of several hundred GHz. The proposed fractional order differentiator is demonstrated experimentally. A Gaussian-like pulse with a bandwidth of about 200 GHz is temporally differentiated with a tunable order range from 0.83 to 1.03.

OCIS codes: (070.1170) Analog optical signal processing; (320.5540) Pulse shaping; (200.4740) Optical processing.

References and links

1. J. Azaña and M. Kulishov, "All-fibre ultrafast optical differentiator based on π phase-shifted long-period grating," Electron. Lett. **41**(25), 1368–1369 (2005).
2. M. Kulishov and J. Azaña, "Long-period fiber gratings as ultrafast optical differentiators," Opt. Lett. **30**(20), 2700–2702 (2005).
3. R. Slavík, Y. Park, M. Kulishov, R. Morandotti, and J. Azaña, "Ultrafast all-optical differentiators," Opt. Express **14**(22), 10699–10707 (2006).
4. R. Slavík, Y. Park, M. Kulishov, and J. Azaña, "Terahertz-bandwidth high-order temporal differentiators based on phase-shifted long-period fiber gratings," Opt. Lett. **34**(20), 3116–3118 (2009).
5. N. K. Berger, B. Levit, B. Fischer, M. Kulishov, D. V. Plant, and J. Azaña, "Temporal differentiation of optical signals using a phase-shifted fiber Bragg grating," Opt. Express **15**(2), 371–381 (2007).
6. M. Kulishov and J. Azaña, "Design of high-order all-optical temporal differentiators based on multiple-phase-shifted fiber Bragg gratings," Opt. Express **15**(10), 6152–6166 (2007).
7. Y. Park, J. Azaña, and R. Slavík, "Ultrafast all-optical first- and higher-order differentiators based on interferometers," Opt. Lett. **32**(6), 710–712 (2007).
8. J. Dong, A. Zheng, D. Gao, L. Lei, D. Huang, and X. Zhang, "Compact, flexible and versatile photonic differentiator using silicon Mach-Zehnder interferometers," Opt. Express **21**(6), 7014–7024 (2013).
9. J. Xu, X. Zhang, J. Dong, D. Liu, and D. Huang, "High-speed all-optical differentiator based on a semiconductor optical amplifier and an optical filter," Opt. Lett. **32**(13), 1872–1874 (2007).
10. J. Xu, X. Zhang, J. Dong, D. Liu, and D. Huang, "All-optical differentiator based on cross-gain modulation in semiconductor optical amplifier," Opt. Lett. **32**(20), 3029–3031 (2007).
11. F. Liu, T. Wang, L. Qiang, T. Ye, Z. Zhang, M. Qiu, and Y. Su, "Compact optical temporal differentiator based on silicon microring resonator," Opt. Express **16**(20), 15880–15886 (2008).
12. J. Dong, A. Zheng, D. Gao, S. Liao, L. Lei, D. Huang, and X. Zhang, "High-order photonic differentiator employing on-chip cascaded microring resonators," Opt. Lett. **38**(5), 628–630 (2013).
13. M. Li, H.-S. Jeong, J. Azaña, and T.-J. Ahn, "25-terahertz-bandwidth all-optical temporal differentiator," Opt. Express **20**(27), 28273–28280 (2012).
14. T.-J. Ahn and J. Azaña, "Wavelength-selective directional couplers as ultrafast optical differentiators," Opt. Express **19**(8), 7625–7632 (2011).
15. H. You, T. Ning, W. Jian, L. Pei, X. Wen, J. Li, and H. Chen, "Optical temporal differentiator using a twin-core fiber," Opt. Eng. **52**(1), 015005 (2013).
16. C. Cuadrado-Laborde, "All-optical ultrafast fractional differentiator," Opt. Quantum Electron. **40**(13), 983–990 (2008).

#212794 - $15.00 USD Received 26 May 2014; revised 4 Jul 2014; accepted 11 Jul 2014; published 21 Jul 2014

17. C. Cuadrado-Laborde and M. V. Andrés, "In-fiber all-optical fractional differentiator," Opt. Lett. **34**(6), 833–835 (2009).
18. M. Li, L.-Y. Shao, J. Albert, and J. Yao, "Continuously tunable photonic fractional temporal differentiator based on a tilted fiber Bragg grating," IEEE Photon. Technol. Lett. **23**(4), 251–253 (2011).
19. H. Shahoei, J. Albert, and J. Yao, "Tunable fractional order temporal differentiator by optically pumping a tilted fiber Bragg grating," IEEE Photon. Technol. Lett. **24**(9), 730–732 (2012).
20. H. Shahoei, D.-X. Xu, J. H. Schmid, and J. Yao, "Photonic fractional-order differentiator using an SOI microring resonator with an MMI coupler," IEEE Photon. Technol. Lett. **25**(15), 1408–1411 (2013).
21. G. T. Reed and A. P. Knights, *Silicon Photonics* (John Wiley, 2004).
22. H. Xu, Z. Li, Y. Zhu, Y. Li, Y. Yu, and J. Yu, "Silicon optical modulator with integrated grating couplers based on 0.18-μm complementary metal oxide semiconductor technology," Opt. Eng. **50**(4), 044001 (2011).
23. T. Yang, J. Dong, L. Liu, S. Liao, S. Tan, L. Shi, D. Gao, and X. Zhang, "Experimental observation of optical differentiation and optical Hilbert transformation using a single SOI microdisk chip," Sci. Rep. **4**, 3960 (2014).

1. Introduction

Temporal photonic differentiator is a basic operator that performs real-time differentiation of the field envelope of an optical signal, which has wide applications in numerous fields such as pulse characterization, ultra-fast signal generation, and ultra-high-speed coding.

Numerous techniques have been proposed recently to implement all-optical temporal differentiation, including the use of a long period fiber grating [1–4], a phase shifted fiber Bragg grating [5, 6], an interferometer [7, 8], a semiconductor optical amplifier [9, 10], a silicon microring resonator [11, 12], or a directional coupler [13–15]. In Ref [16], Cuadrado-Laborde *et al* explored fractional differentiation for the first time, and presented an all-optical temporal differentiator using a photonic Mach-Zehnder interferometer (MZI) by numerical simulations, but the tunability of the differentiation order was not mentioned. Afterwards, the fractional-order differentiator has been implemented based on different methods such as asymmetrical phase-shifted fiber Bragg grating [17], tilted fiber Bragg grating [18, 19], and silicon-on-isolator (SOI) microring resonator with a multimode interferometer (MMI) coupler [20], and the last two schemes could provide tunability of fractional order. Fractional differentiation can be considered as a generalization of integer-order differentiation, with potentials to accomplish what integer-order differentiation cannot [16].

In this paper, we demonstrate a tunable fractional-order differentiator based on an electrically tuned SOI MZI. Our scheme has a large operation bandwidth of several hundred GHz. By changing the voltage applied on one arm of the MZI, the waveguide loss of the arm is changed correspondingly, which leads to the variation of phase shift at the resonance wavelength. This means the fractional-order differentiation is possible and the differentiation order is also tunable. A Gaussian-like pulse with a bandwidth of about 200 GHz is successfully differentiated with a tunable fractional order ranging from 0.83 to 1.03. Our scheme provides an integrated solution for fractional order differentiation.

2. Operation principle

An *N*th-order temporal differentiator provides the *N*th-order derivation of the complex envelope of an input optical signal. Therefore, the output differentiated signal in frequency domain can be written by

$$E_{out}(\omega) = \left[j(\omega - \omega_0) \right]^N E_{in}(\omega) \tag{1}$$

where N is not necessarily an integer generalized to fractional-order differentiation, ω and ω_0 are the optical frequency and the carrier frequency, E_{in} and E_{out} are the input and output optical fields, respectively. Thus one needs to design a frequency response of $\left[j(\omega - \omega_0) \right]^N$ to implement the differentiation.

For an asymmetric MZI, the spectral transfer function is given by

$$H(\omega) = 1 + \beta \exp[\mathrm{j}(\omega\tau + \varphi_0)] \tag{2}$$

#212794 - $15.00 USD Received 26 May 2014; revised 4 Jul 2014; accepted 11 Jul 2014; published 21 Jul 2014

where β is determined by the power splitting ratio of two arms of MZI, τ and φ_0 are the relative time delay and phase difference between the two arms, respectively.

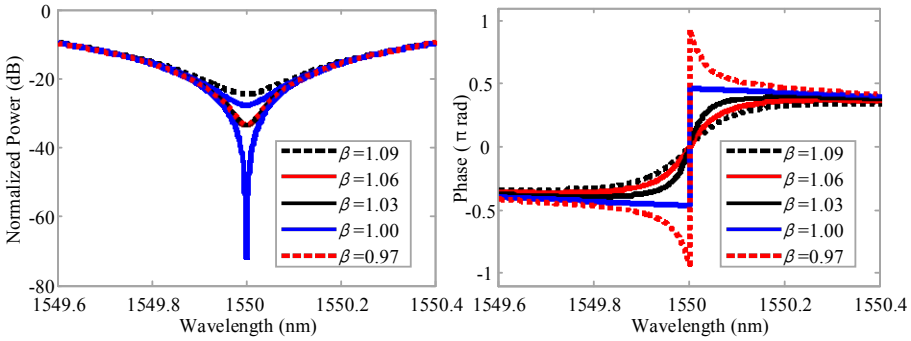

Fig. 1. The magnitude (a) and phase response (b) of the MZI operating at 1550 nm for different value of β .

By changing the voltage applied on one arm of the MZI, we can change the value of the power splitting ratio β [21]. Figs. 1(a) and 1(b) show the responses of amplitude and phase of MZI at different splitting ratio. The MZI structure has a good linear frequency response near its resonant frequency notch when $\beta = 1$, which exactly act as the first-order differentiator [7]. As can be seen in Fig. 1(b), the phase shift is less than π when $\beta >1$, and higher than π when $\beta <1$, corresponding to the fractional order differentiator.

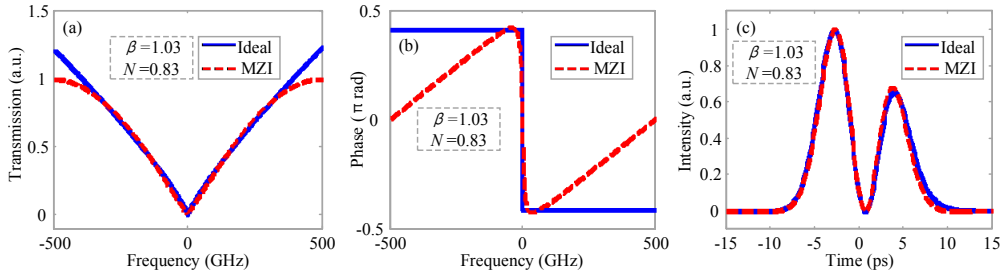

Fig. 2. (a) The amplitude response and (b) the phase response of the transmission spectrum of the MZI with β = 1.03. The solid lines shows the magnitude and phase response of an ideal differentiator. (c) Simulated output pulse from the MZI. The solid line shows the output pulse from an ideal differentiator. The fractional order is 0.83.

Figures 2(a) and 2(b) show the amplitude and phase responses of an MZI with β = 1.03 corresponding to differentiator with a fractional order of 0.83. Figure 2(c) simulates the output differentiated waveform with the MZI, which accords well with the ideal fractional-order differentiation with an order of 0.83. Therefore, the MZI with two arms unbalanced can implement fractional order differentiation.

We then employ on-chip MZI structure to implement fractional-order differentiation. The device was fabricated at the SMIC commercial 0.18μm CMOS foundry [22]. We use a silicon-on-insulator (SOI) wafer with 340 nm top silicon layer and 2 μm buried oxide layer. The straight rib waveguides and multimode interference (MMI) couplers are patterned by deep UV lithography and then dry etched to form 50nm thick slabs. Boron and Phosphor implantations are followed to form the PN junctions. For metal-silicon contact, highly P and N type doping with density of 1×10^{19}cm^{-3} are located 700 nm away from the waveguide side wall. This distance comes from a tradeoff between modulation bandwidth and optical absorption loss. At last, aluminum layer with 1μm thickness is sputtered, patterned and etched down as the electrodes with the ground-signal-ground pads. Figure 3 shows the micrographs

#212794 - $15.00 USD Received 26 May 2014; revised 4 Jul 2014; accepted 11 Jul 2014; published 21 Jul 2014

of (a) total MZI structure, (b) coupling grating, (c) MMI, and (d) integrated *p-i-n* diode. The scaling bars are shown.

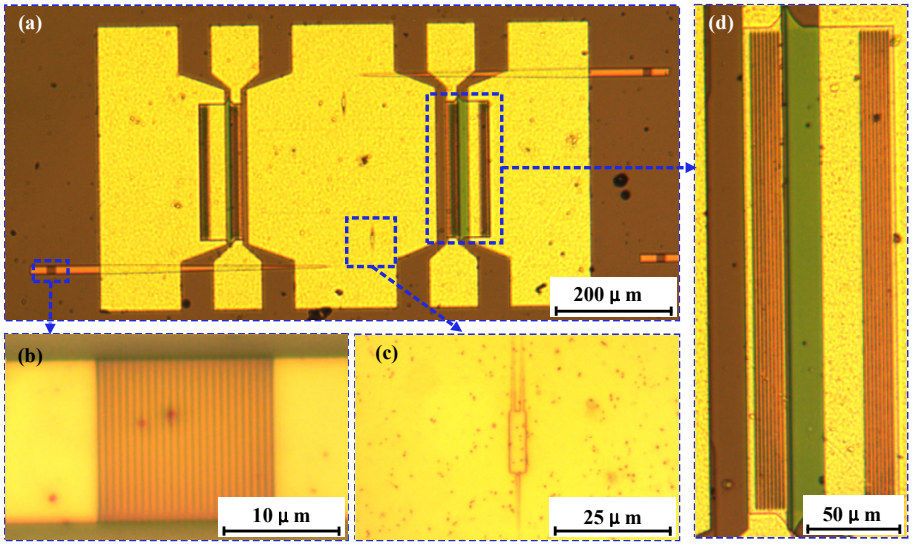

Fig. 3. Micrographs of (a) MZI, (b) coupling grating, (c) MMI, (d) integrated *p-i-n* diode.

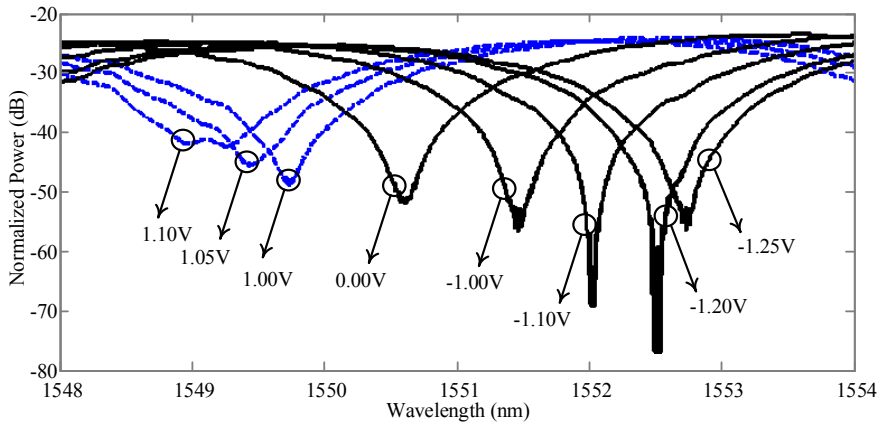

Fig. 4. Measured transfer functions of the MZI at different voltages, zigzag line (positive voltages): voltages applied on Arm A, solid line: without voltage, dash and dot line: voltages applied on Arm B.

Figure 4 shows the measured transfer function of the MZI. We apply different voltages on two arms of the MZI. Voltages applied on one arm (marked as Arm A) of the MZI are defined as positive voltages (dash line) in Fig. 4, and voltages applied on another arm (marked as Arm B) are defined as negative voltages (solid line). Comparing the amplitude responses of Fig. 1(a) and Fig. 4, we can see that when the applied voltage is −1.2V, there is the deepest frequency notch, indicating $\beta = 1$ and a π phase shift at the frequency notch. On the other hand, the phase shift of the MZI is less or more than π when applying the other voltages. When the voltage is changed by 0.1V, the resonance wavelength is shifted by about 0.5nm correspondingly. Therefore the optical carrier of input signal should be tuned correspondingly. The total loss (including the coupling loss and transmission loss) of the MZI chip is about 24dB. The free spectral range (FSR) is 700 GHz and the 3-dB bandwidth is about 550 GHz. Thus the differentiator is expected to have an operation bandwidth of several

#212794 - $15.00 USD Received 26 May 2014; revised 4 Jul 2014; accepted 11 Jul 2014; published 21 Jul 2014

hundred GHz. The notch depth ranges from 15 dB to 40dB when applying different voltages. Due to the hardware restraint, the phase response of the MZI chip was not measured. However, we can deduce from Fig. 1 and Fig. 4 that the MZI has a varied phase shift at the resonant frequency by applying different voltages.

3. Experiment and results

The experimental setup is shown in Fig. 5. The tunable pulse generator is composed of a tunable laser source (TLS), two polarization controllers (PCs), a Mach-Zehnder modulator (MZM) to produce a direct current (DC) free pulse train, an erbium doped fiber amplifier (EDFA) to compensate the loss induced by the MZM, an optical tunable delay line (OTDL) used to synchronize the radio frequency (RF) applied on the MZM and phase modulator (PM), a PM to induce large chirp, a segment of single mode fiber (SMF) for chirp compression to generate a short pulse train [23]. The pulse generator generate a Gaussian-like pulse train with a full width at half maximum (FWHM) of 5.4 ps and a repetition frequency of 10 GHz. The Gaussian-like pulse is shown in Fig. 6(a). The output signal of the MZI chip is amplified by an EDFA and then analyzed through a high speed oscilloscope (OSO) with a bandwidth of 500GHz (EYE-1100C).

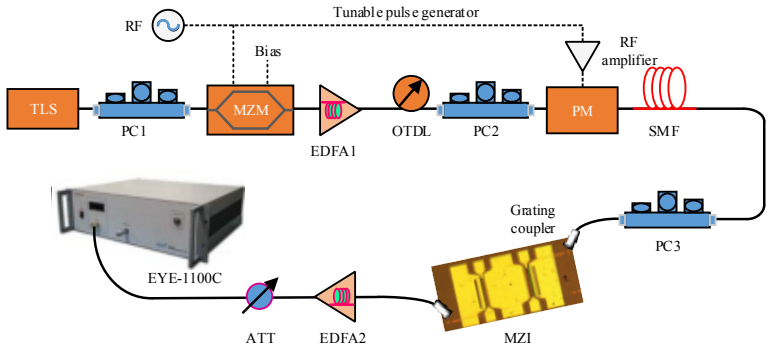

Fig. 5. Experimental setup for the fractional order differentiator with on chip MZI structure.

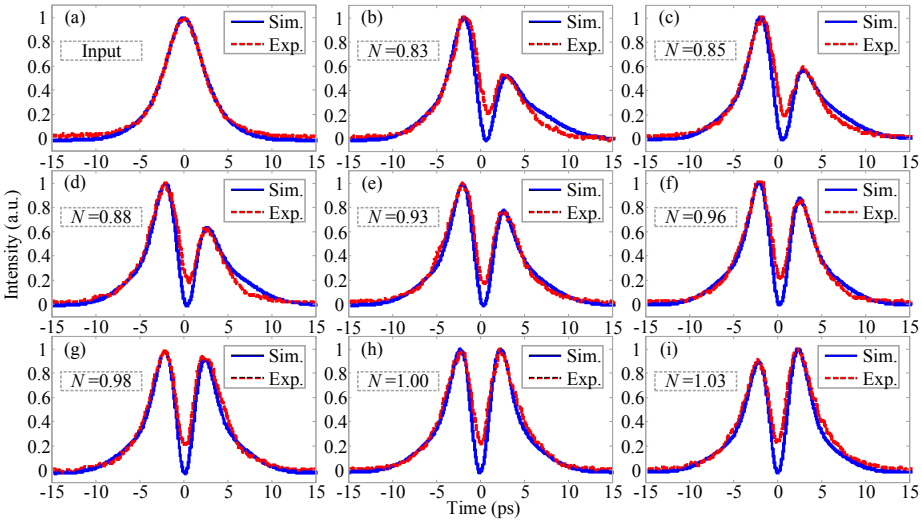

Fig. 6. (a) An input Gaussian-like pulse with an FWHM of 5.4 ps, and the differentiated pulses at the different voltages corresponding to differentiation orders of (b) N = 0.83, (c) N = 0.85, (d) N = 0.88, (e) N = 0.93, (f) N = 0.96, (g) N = 0.98, (h) N = 1.00, (i) N = 1.03.

#212794 - $15.00 USD Received 26 May 2014; revised 4 Jul 2014; accepted 11 Jul 2014; published 21 Jul 2014

When we apply voltages with 1.10V, 1.05V, 1.00V, 0V, −1.00V, −1.10V, −1.20V, −1.25V on the MZI, and fine tune the TLS wavelength to be aligned with the notch wavelength, the output differentiated waveforms are shown in Figs. 6(b)–6(i). At the same time, the simulated waveforms of fractional-order differentiation are also shown, whose fractional orders are N = 0.83, 0.85, 0.88, 0.93, 0.96, 0.98, 1.00, 1.03, respectively. One can see there is a good agreement between the measured pulses and the ideal differentiators except a small discrepancy at the pulse notch. In order to align the laser wavelength to the spectral notch, we first observe the MZI spectral notch and fix it. For example, Fig. 7 shows the spectra of input Gaussian-like pulse and the output pulse with a differentiation order of 1.00. The notch wavelength is about 1552.5 nm. Then we tune the laser wavelength at the same wavelength. With the tunable pulse generator in Fig. 5, we obtain a Gaussian pulse train whose spectrum is shown in Fig. 7 (blue line). The spectrum is not Gaussian-like just because it is chirped with the tunable pulse generator. Finally, the spectrum after the MZI chip is observed as shown in Fig. 7 (red line). One can see the input signal carrier is well aligned with the MZI resonant notch, and the carrier is deeply suppressed at the output spectrum.

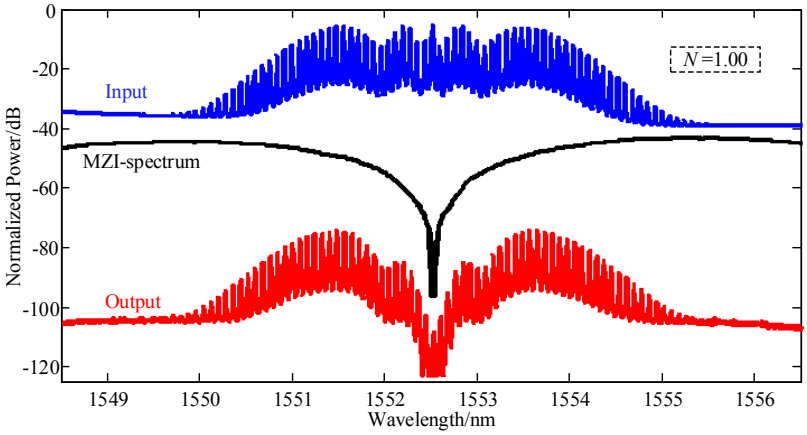

Fig. 7. Measured spectra of input Gaussian-like pulse and the output pulse.

We may notice that the MZI functions as a fractional differentiator with N = 0.93 when no voltage is applied. This is caused by the device fabrication imperfection, which leads to the unequal power of the two arms of the MZI. By improving the fabrication performance, we can implement a differentiator with N = 1 at the voltage of zero, and then obtain fractional order N >1 with negative voltages applied, and obtain N <1 with positive voltages. But the fractional order range is limited by the protection voltage of the MZI in case of damaging.

4. Conclusions

A silicon photonics-based continuously tunable fractional-order temporal differentiator was proposed and experimentally demonstrated. The key to achieve the differentiation order tuning was based on the changing of the voltage applied on the MZI arms, which led to the change of the waveguide loss, hence change of the phase shift. We successfully demonstrated fractional order differentiation of a 5.4-ps Gaussian-like pulse. The fractional order is varied from 0.83 to 1.03.

Acknowledgments

This work was partially supported by the National Natural Science Foundation of China (Grant No. 60901006, Grant No. 11174096), National Basic Research Program of China (Grant No. 2011CB301704), and the Program for New Century Excellent Talents in Ministry of Education of China (Grant No. NCET-11-0168), the National Natural Science Foundation of China (Grant No. 60901006, and Grant No. 11174096), and the Fundamental Research Funds for the Central Universities, HUST: 2014YQ015.